Journal of Metals, Materials and Minerals, 36(3), e2610, 2026

Enhancing aqueous solubility of a psoralen derivative via cyclodextrin inclusion complexation: In silico and *in vitro* study

Gulzaib BASHARAT[1], Saba ALI[2], Pattharamon CHAIKHUN[2], Choosak JAROENRIT[3], Kuakarun KRUSONG[2], Thanthapatra BUNCHUAY[4], Tanatorn KHOTAVIVATTANA[3], and Thanyada RUNGROTMONGKOL[1,2,*]

[1] *Program in Bioinformatics and Computational Biology, College of Interdisciplinary and Integrative Studies, Chulalongkorn University, Bangkok 10330, Thailand*

[2] *Center of Excellence in Structural and Computational Biology, Department of Biochemistry, Faculty of Science, Chulalongkorn University, Bangkok 10330, Thailand*

[3] *Center of Excellence in Natural Products Chemistry, Department of Chemistry, Faculty of Science, Chulalongkorn University, Bangkok 10330, Thailand*

[4] *Department of Chemistry, Faculty of Science, Mahidol University, Bangkok, Thailand*

***Corresponding author e-mail**: thanyada.r@chula.ac.th

Received date:
23 December 2025
Revised date:
17 April 2026
Accepted date:
4 June 2026

Keywords:
Psoralen derivative;
β-Cyclodextrins;
Inclusion complex;
Computational study;
Experimental validation

Abstract

N-(4-Bromobenzoyl)-8-methoxypsoralen-4-amine (BNB) is a psoralen derivative with potent cytotoxic activity against breast cancer cells but with limited pharmaceutical application and therapeutic potential due to its extremely low aqueous solubility. To overcome this limitation, β-cyclodextrin (βCD) and its derivatives dimethyl-βCD (DMβCD), hydroxypropyl-βCD (HPβCD), and sulfobutylether-βCD (SBEβCD) were investigated as carriers to enhance BNB's aqueous solubility via cyclodextrin inclusion complexation. A combined computational–experimental strategy was employed, integrating molecular docking, 500-ns all-atom molecular dynamics simulations in quintuplicate runs (2.5 μs in total), and experimental validation by phase solubility analysis, scanning electron microscopy (SEM), and differential scanning calorimetry (DSC). Docking and simulations revealed stable host–guest interactions, with SBEβCD showing the most favorable binding free energies, the highest number of atomic contacts, and the lowest solvent-accessible surface area, indicative of deep and stable encapsulation. Phase solubility studies corroborated these findings, with BNB/SBEβCD exhibiting the highest apparent stability constant. The formation of the inclusion complex was further supported by SEM and DSC, which revealed pronounced morphological changes and thermal evidence consistent with encapsulation, including suppression of the BNB melting endotherm. ^{1}H NMR spectroscopic analysis further confirmed complex formation through observed peak broadening and chemical shift perturbations upon complexation. Collectively, these results identify SBEβCD as a highly effective carrier for BNB, offering a rational approach to improve solubility through stable complex formation, and supporting its potential as a promising chemotherapeutic candidate for breast cancer treatment.

1. Introduction

Breast cancer remains a significant global public health concern [1]. According to international cancer statistics, it is the most frequently diagnosed cancer and, although rare, can also occur in men [2]. The etiology of breast cancer involves a complex interplay of genetic, behavioral, and environmental factors [3]. Among current therapeutic approaches, chemotherapy is one of the most effective treatments for different cancer stages and subtypes [4]. However, high-dose chemotherapy often results in severe adverse effects and the development of chemoresistance in cancer cells [5]. Therefore, developing novel chemotherapeutic agents with potent anti-breast cancer activity and reduced systemic toxicity is critical for improving clinical outcomes.

N-(4-Bromobenzoyl)-8-methoxypsoralen-4-amine (BNB) is a psoralen derivative synthesized by substituting a benzamide moiety onto 8-methoxypsoralen (8-MOP) Figure 1(a). BNB has demonstrated promising anti-breast cancer activity in both irradiated and non-irradiated conditions. It exerts cytotoxic effects on multiple breast cancer cell lines, including MDA-MB-231, T47-D, and SK-BR-3, with the highest potency observed against T47-D cells (IC50 = 10.14 μM). This efficacy is comparable to or greater than that of reference drugs such as doxorubicin (1.46 μM), tamoxifen citrate (20.86 μM), and lapatinib (9.78 μM). However, the practical application of BNB is limited by its extremely low aqueous solubility (ESOL Log Sf = –5.09) [6], which markedly limits its bioavailability.

Cyclodextrins (CDs) Figure 1(b) are cyclic oligosaccharides of α-D-glucopyranose units linked by α-1,4 glycosidic bonds, forming a truncated cone-shaped structure. The inner cavity of CDs is hydrophobic, while the outer surface is hydrophilic, enabling their use as molecular hosts in inclusion complex formation. CDs are produced

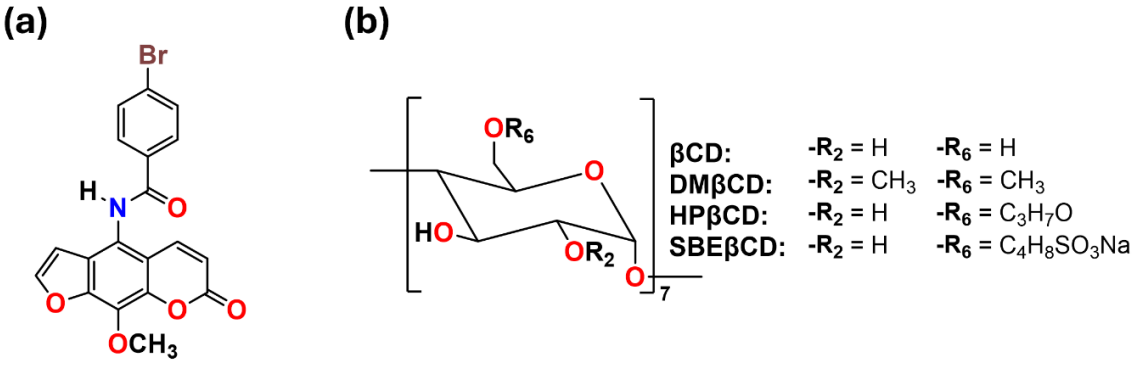

Figure 1. Chemical structures of (a) N-(4-bromobenzoyl)-8-methoxypsoralen-4-amine (BNB), and (b) β-cyclodextrin (βCD) with its derivatives: di-O-methyl-β-cyclodextrin (DMβCD), hydroxypropyl-β-cyclodextrin (HPβCD), and sulfobutylether-β-cyclodextrin (SBEβCD). Substituent groups at positions R2 and R6 are indicated.

enzymatically from starch using cyclodextrin glycosyltransferase [7,8]. The three naturally occurring CDs α-cyclodextrin (α-CD), β-cyclodextrin (β-CD), and γ-cyclodextrin (γ-CD) vary in the number of glucose units and internal cavity size [9]. Cyclodextrins have been widely used in the pharmaceutical industry due to their ability to form host-guest inclusion complexes with poorly water-soluble compounds that match the shape and size of their hydrophobic cavity. These complexes are stabilized through hydrogen bonding, van der Waals forces, and hydrophobic interactions [10]. CDs' dual hydrophilic-hydrophobic nature allows them to enhance the solubility and stability of drug molecules. βCD is among the most commonly used cyclodextrins due to its optimal cavity size, good biocompatibility, wide availability, and cost-effectiveness [11,12]. Several derivatives of βCD, such as di-O-methyl-β-cyclodextrin (DMβCD), hydroxypropyl-β-cyclodextrin (HPβCD), and sulfobutylether-β-cyclodextrin (SBEβCD), have been developed to improve solubility and complexation efficiency further [13].

In this context, the present study aims to improve the aqueous solubility and physicochemical stability of BNB through inclusion complexation with βCD and its derivatives (DMβCD, HPβCD, and SBEβCD). A combination of computational modelling and experimental techniques, including phase solubility analysis, SEM, and DSC, was employed to elucidate the interaction mechanisms and confirm complex formation. These findings provide a foundation for the potential pharmaceutical development of BNB with enhanced biopharmaceutical properties.

2. Materials and methods

2.1 Computational details

2.1.1 System preparation

The three-dimensional structure of BNB was constructed in GaussView 6.0 and optimized at the Hartree-Fock (HF) level with the 6-31G* basis set, as implemented in Gaussian 16 [14]. The neutral form of BNB at physiological pH (7.0) was confirmed using Marvin Sketch, and this structure was employed in subsequent molecular dynamics (MD) simulations [15]. As host molecules, we considered β-cyclodextrin (βCD) and three derivatives: di-O-methyl-β-cyclodextrin (DMβCD, DS = 14), hydroxypropyl-β-cyclodextrin (HPβCD, DS = 4), and sulfobutylether-β-cyclodextrin (SBEβCD, DS = 7). The structures of βCD and its derivatives were constructed from canonical models of seven α-D-glucopyranose units connected by α-1,4-glycosidic bonds, yielding the characteristic truncated-cone geometry of cyclodextrins. Substitutions were positioned according to experimental reports: in DMβCD, methyl groups were placed on both the O2 and O6 hydroxyl sites; in HPβCD, four hydroxypropyl groups were attached at the O6 positions on the primary rim [10]; and in SBEβCD, seven sulfobutylether groups were substituted at O6 [16].

2.1.2 Molecular docking

Molecular docking of BNB with βCDs was carried out using the CDOCKER module in Accelrys Discovery Studio 2.5 (Accelrys Software Inc., San Diego, CA, USA). Docking was performed within a 10 Å sphere centered on the cyclodextrin cavity to capture the full range of potential inclusion orientations. For each host-guest system, the top 100 poses were retained. Binding preferences were quantified by calculating the percentage of docked conformations (%DCs) adopting each orientation, providing a measure of conformational consistency. Among the generated poses, the lowest-energy complex was selected as the most favorable binding geometry. These minimum-energy conformations of the BNB/βCD inclusion complexes were subsequently employed as starting structures for molecular dynamics (MD) simulations.

2.1.3 All-atom molecular dynamics simulations

MD simulations were employed to investigate the structural dynamics of the BNB/βCD inclusion complexes using AMBER22 [17] The GLYCAM-06 force field [18] was used for βCDs, and AMBER force field (GAFF) [19] was applied to BNB. Systems were solvated in explicit water using the TIP3P model [20], with a 15 Å buffer surrounding all solutes. Energy minimization was performed in two stages: 1,000 steps of steepest descent followed by 3,000 steps of conjugate gradient minimization for solvent molecules, and then for the whole system. Simulations were run under periodic boundary conditions with a 2-fs time step. Bond lengths involving hydrogen were constrained using SHAKE [21] and long-range electrostatics were treated with the Particle Mesh Ewald method [22] using a 12 Å cutoff. Each system was heated from 10 K to 298 K over 100 ps, followed by production MD in the NPT ensemble (1 atm, 298 K).

For each complex, five independent 500 ns simulations (MD#1–5) were performed, and the final 100 ns from each trajectory were used for analysis. Structural stability was assessed via root-mean-square deviation (RMSD). To monitor inclusion geometry, distances were measured between the BNB and center of mass of βCD primary rim. Host-guest interactions were quantified by counting atom-atom contacts within 3.0 Å. Encapsulation efficiency and solvent exposure were evaluated from solvent-accessible surface area (SASA) calculations. Binding affinity was estimated using MM/GBSA and MM/PBSA free energy calculations providing a comprehensive view of the energetic landscape and thermodynamic stability of the complexes.

2.2 Experimental details

2.2.1 Chemical reagents

BNB was synthesized via a 3-step protocol from 8-MOP based on the literature procedure [6]. Briefly, nitration of 8-MOP using nitric acid in glacial acetic acid gave the nitro derivative as a yellow solid (98 %yield). Reduction of the nitro product using tin powder and conc. HCl in methanol gave the amino derivative as a yellow solid (74 %yield). Lastly, alkylation of the amino compound using 4-bromobenzoyl chloride and K_2CO_3 in dichloromethane gave BNB as a yellow solid (730 mg, 59 %yield). β-cyclodextrin (βCD), hydroxy-propyl-β-cyclodextrin (HPβCD) and sulfobutylether-β-cyclodextrin (SBEβCD) were purchased from FUJIFILM Wako Pure Chemical Corporation (Osaka, JAPAN).

2.2.2 Phase solubility study

Phase solubility studies were performed following the method of Higuchi and Connors [23]. Briefly, an excess amount of BNB (2 mg) was added to aqueous solutions of βCDs at concentrations ranging from 0 mM to 10 mM. Samples were vortexed for uniform dispersion and incubated under constant agitation (250 rpm) at 25°C for 72 h. After equilibration, suspensions were centrifuged at 12,000 rpm for 15 min, and the supernatants were filtered through 0.45 µm membranes. Filtrates were diluted (1:1, v/v, ethanol-water), and absorbance was measured at 260 nm. Phase solubility diagrams were constructed to evaluate host-guest interactions. The apparent stability constant (K_c) was calculated according to Equation (1), where S_0 represents the intrinsic solubility of BNB in water at 25°C in the absence of cyclodextrins.

$$K_c = \frac{\text{slope}}{S_0\,(1-\text{slope})} \quad (1)$$

2.2.3 Inclusion complex preparation

Inclusion complexes of BNB with β-cyclodextrins (βCDs) were prepared via lyophilization reported as more reliable method than kneading method for obtaining homogeneous inclusion complexes [24–26]. A 1:1 stoichiometric ratio, determined from phase solubility studies, was employed. Equimolar solutions (1 mM) of BNB and the respective βCDs were dissolved in 50 mL of water and stirred for 24 h to ensure complete complexation. The suspensions were subsequently centrifuged at 12,000 rpm for 15 min and filtered through 0.45 µm membranes. The resulting filtrates were frozen at –80°C overnight and freeze-dried for 72 h using a Lyovapor L-200 lyophilizer. The dried complexes were collected as powders and stored in a desiccator to maintain stability for further experiments. For comparison, physical mixtures were prepared by combining BNB and βCDs in a 1:1 molar ratio, followed by geometric mixing at room temperature (25°C) until a visually homogeneous powder blend was obtained. No solvent or additional mechanical treatment was applied. The resulting physical mixtures were used as controls to distinguish inclusion complex formation from simple mixing.

2.2.4 Characterization of inclusion complexation

2.2.4.1 Scanning electron microscope (SEM)

The surface morphology of pure BNB, β-cyclodextrins (βCDs), BNB/βCDs inclusion complexes, and their corresponding physical mixtures were examined using a scanning electron microscope (JEOL JSM-IT300). For analysis, 1 mg to 2 mg of each sample was mounted on aluminum stubs and coated with a thin layer of gold to enhance conductivity. Micrographs were captured at multiple magnifications using an accelerating voltage of 12.5 kV to assess morphological characteristics and surface features.

2.2.4.2 Differential scanning calorimetry (DSC)

Thermal characterization of pure BNB, β-cyclodextrins (βCDs), BNB/βCDs inclusion complexes, and physical mixtures were performed using a differential scanning calorimeter (NETZSCH DSC 204F1 Phoenix). Approximately 3 mg to 5 mg of each sample was sealed in an aluminum pan and heated from 25°C to 300°C at a rate of $10°C \cdot min^{-1}$. Nitrogen was used as a purge gas at a flow rate of $25\ mL \cdot min^{-1}$ throughout the analysis. Thermograms were analyzed to assess thermal properties and to infer interactions between BNB and βCDs.

2.2.4.3 ^{1}H-NMR spectroscopic analysis

^{1}H NMR spectra were recorded on a 400 MHz NMR spectrometer using DMSO-d_6 as the deuterated solvent. Samples were prepared by dissolving free BNB, cyclodextrins (βCD, HPβCD, and SBEβCD), and their corresponding BNB/βCDs complexes separately in DMSO-d_6 at appropriate concentrations. All spectra were acquired at ambient temperature, and chemical shifts (δ) are reported in parts per million (ppm) referenced to the residual solvent signal of DMSO-d_6 (δ 2.50 ppm). The spectra of the free BNB, cyclodextrins, and BNB/βCDs complexes were compared to evaluating chemical shift perturbations and changes in peak characteristics indicative of host-guest complex formation.

3. Results and discussion

3.1 Possible binding modes of BNB with βCDs

Molecular docking was performed to investigate how BNB could fit within the cavities of βCD and their derivatives DMβCD,

HPβCD, and SBEβCD. From the docking results show in Figure 2, two predominant orientations are observed: B-form, where the bromobenzene moiety enters the CD cavity, and C-form, where the methoxypsoralen moiety is inserted. The relative population of each form is indicated in blue (DC, %), and the corresponding average binding energy (ΔE, kcal·mol^{-1}) is shown in red. Among the complexes, BNB/SBEβCD displayed the most favorable binding energies (–36.95 and –35.50 kcal·mol^{-1} for B- and C-forms, respectively). Both BNB/βCD and BNB/HPβCD displayed mixed populations of B- and C-forms but with weaker binding affinities, whereas BNB/DMβCD consistently adopted only the B-form. These complexes were used as the starting structures for performing MD simulations in aqueous solution.

3.2 System stability and dynamics

The structural stability of the BNB/βCD inclusion complexes was assessed by monitoring the all-atom root-mean-square deviation (RMSD) relative to the initial structure across five independent 500 ns MD simulations Figure 3. For the BNB/βCD complex, both orientations exhibited frequent conformational fluctuations in four out of five replicates, suggesting poor accommodation of the guest within the cavity. For the B-form simulations, dissociation occurred at ~383 ns (MD1), 220 ns to 290 ns (MD2), 19 ns to 82 ns and 137 ns (MD3), and multiple intervals between 12 ns to 329 ns (MD4). Notably, the B-form in MD2–4 subsequently converted to the C-form, consistent with the sharp RMSD transitions observed in Figure 3. Conversely, for the C-form simulations, dissociation was detected at 57 ns to 226 ns (MD1), 168 ns to 442 ns (MD2), 26 ns to 478 ns (MD3), and 21 ns to 377 ns (MD4). In MD3 and MD4, these C-form insertions were converted to the B-form, further confirming the reciprocal instability of both orientations. These results highlight that, while both forms can transiently occupy the cavity, frequent orientation switching and early dissociation events underscore the weak and unstable binding of BNB in native βCD. Overall, across ten MD simulations of the BNB/βCD complex, the B- and C-form insertions were counted as four and six, respectively. Dissociation and reassociation of host-guest complexation were found in the previous studies [16,27].

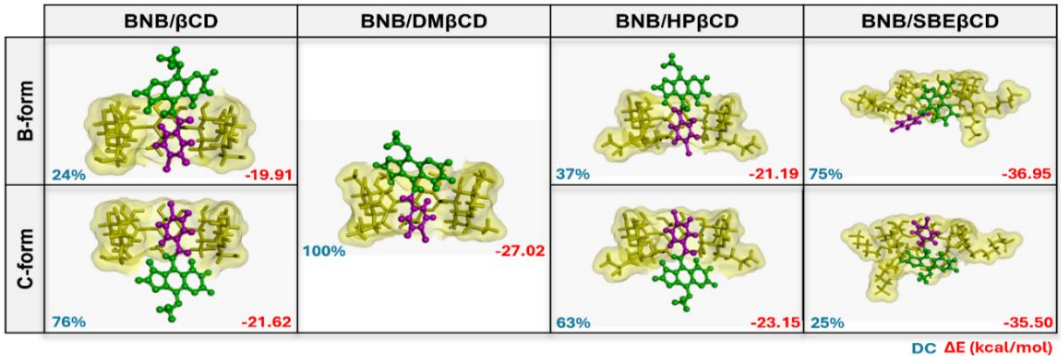

Figure 2. Representative docked complexes of BNB with βCDs in B- and C-form conformations. %Docked conformations (%DC) are shown in blue, and the corresponding interaction energies (ΔE, kcal·mol^{-1}) are shown in red, highlighting the preferred binding orientations and relative stabilities of BNB within the cyclodextrin cavities.

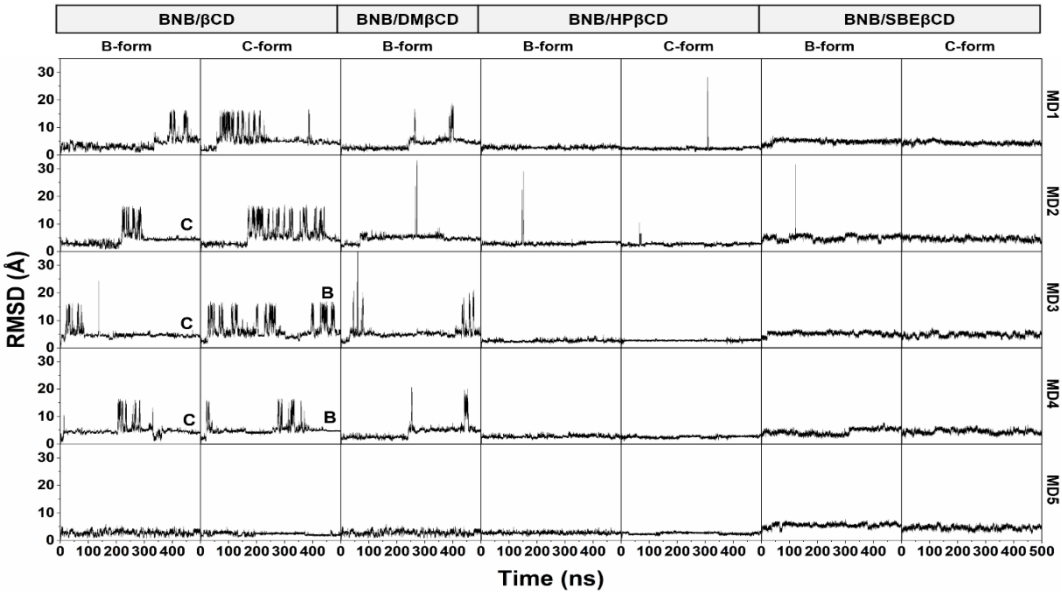

Figure 3. All-atom RMSD plots for BNB/βCDs inclusion complexes in B-form and C-form insertions were analyzed for 500 ns in quintuplicate runs (MD1-5). In several trajectories of the BNB/βCD complex, dissociation events were accompanied by reorientation of the guest molecule, leading to transitions between B-form and C-form orientations and *vice versa*. By contrast, such transitions were not observed in complexes with DMβCD, HPβCD, or SBEβCD.

A comparable trend was observed for the BNB/DMβCD complex, although the fluctuations occurred within a narrower time window compared with βCD. The dissociation was identified at 262 ns to 267 ns and 396 ns to 402 ns (MD1), 267 ns to 272 ns (MD2), 43 ns to 82 ns and 430 ns to 470 ns (MD3), and 241 ns to 329 ns (MD4). Unlike βCD, these events were followed by spontaneous reassociation of the guest without orientation switching, indicating that the B-form is the more favorable configuration for BNB/DMβCD inclusion complexes. By contrast, BNB/HPβCD and BNB/SBEβCD complexes demonstrated markedly greater stability in both B- and C-forms. In these systems, the RMSD traces remained consistently low with minimal deviations across all replicates, indicative of strong host–guest interactions and a reduced likelihood of ligand displacement. Occasional spikes were observed but relaxed rapidly, reflecting transient local rearrangements rather than complete dissociation. These findings are consistent with docking-derived interaction energies, further supporting that SBEβCD and HPβCD form more stable inclusion complexes with BNB compared to native βCD or DMβCD under dynamic conditions. For subsequent analyses, we used snapshots from the final 100 ns of the stable trajectories, excluding MD1 of the B-form and MD2–MD3 of the BNB/βCD C-form because of their persistent instability.

3.3 Host-guest contacts and solvent accessibility

The interaction patterns of BNB with βCD and its derivatives were further examined by analyzing the number of contacts between host and guest, as well as the solvent-accessible surface area (SASA) of BNB, over the final 100 ns of each MD replicate Table 1. Among all systems, the strongest interactions were observed with SBEβCD, which consistently exhibited the highest number of contacts and the lowest SASA values in both orientations. BNB/SBEβCD consistently exhibited the highest number of contacts in both B-form (ranging 43 to 53 contacts) and C-form (approximately 40 to 50 contacts), indicating the strongest and most extensive host-guest interactions. This enhanced interaction likely arises from the bulky sulfobutylether substituents, which increase the cavity's flexibility and provide additional opportunities for van der Waals contacts and hydrogen bonding, consistent with previous observations in piperine/βCD systems [28]. Both orientations were observed for HPβCD, with the C-form showing relatively higher contact numbers and slightly lower SASA values than the B-form, consistent with deeper insertion of the methoxypsoralen moiety. In contrast, native βCD and DMβCD formed fewer contacts and high SASA values overall, indicating weak encapsulation and poor shielding of BNB from solvent particularly DMβCD.

3.4 Thermodynamics profile

MM/GBSA and MM/PBSA calculations (MD5, Table 2) provide insights into the binding energetics of BNB with βCD, DMβCD, HPβCD, and SBEβCD, considering both B- and C-form orientations.

Table 1. Average number of contacts and solvent-accessible surface area (SASA, Å^2) of BNB in complex with βCD and its derivatives (DMβCD, HPβCD, and SBEβCD) for B- and C-form orientations across five independent 500 ns MD simulations. Values are reported as mean ± standard deviation over the final 100 ns of each trajectory.

	Number of contacts		SASA (Å^2)	
	B-form	**C-form**	**B-form**	**C-form**
MD1				
BNB/βCD	NA	34.93 ± 9.84	NA	219.62 ± 31.18
BNB/DMβCD	34.88 ± 11.3	ND	232.91 ± 27.52	ND
BNB/HPβCD	29.58 ± 11.87	37.85 ± 9.85	220.77 ± 37.49	193.85 ± 22.46
BNB/SBEβCD	53.82 ± 15.36	50.61 ± 9.81	148.01 ± 30.18	149.48 ± 23.04
MD2				
BNB/βCD	36.98 ± 9.05^C	NA	221.15 ± 24.08	NA
BNB/DMβCD	39.10 ± 8.59	ND	222.75 ± 16.75	ND
BNB/HPβCD	54.38 ± 11.07	37.39 ± 9.44	169.29 ± 24.51	198.92 ± 20.12
BNB/SBEβCD	43.22 ± 12.86	40.91 ± 12.52	164.56 ± 24.39	168.45 ± 34.96
MD3				
BNB/βCD	43.07 ± 10.48^C	NA	205.36 ± 23.27	NA
BNB/DMβCD	NA	ND	NA	ND
BNB/HPβCD	34.56 ± 12.54	36.18 ± 8.79	209.58 ± 34.79	201.59 ± 16.43
BNB/SBEβCD	46.63 ± 11.04	39.86 ± 10.35	161.96 ± 25.49	184.65 ± 27.01
MD4				
BNB/βCD	41.84 ± 10.68^C	37.88 ± 10.95	206.11 ± 25.95	206.28 ± 22.35
BNB/DMβCD	NA	ND	NA	ND
BNB/HPβCD	31.95 ± 12.88	36.74 ± 8.76	216.46 ± 37.91	193.26 ± 22.06
BNB/SBEβCD	43.88 ± 11.34	44.43 ± 11.84	164.40 ± 25.98	157.36 ± 36.32
MD5				
BNB/βCD	31.63 ± 10.11	39.70 ± 10.62^B	230.86 ± 35.80	206.74 ± 20.40
BNB/DMβCD	30.22 ± 11.53	ND	242.81 ± 47.10	ND
BNB/HPβCD	35.90 ± 10.93	35.87 ± 9.27	221.05 ± 36.53	199.34 ± 18.60
BNB/SBEβCD	49.90 ± 10.69	44.15 ± 12.17	154.32 ± 23.63	151.86 ± 37.14

"B" and "C" stand for B-form and C-form resulting from dissociation of the BNB/βCD complex upon simulations. "ND" indicates that the stable corresponding form was not detected, while "NA" indicates that the form was not applicable to the given system.

Table 2. MM/GBSA and MM/PBSA binding free energy components of BNB/βCDs complexes for B- and C-forms over last 100ns of MD5 (mean ± SD).

	TΔS	ΔE_{vdw}	ΔE_{ele}	MM/GBSA			MM/PBSA		
				$\Delta G_{sol,polar}$	$\Delta G_{sol,non-polar}$	$\Delta G_{bind}^{MM/GBSA}$	$\Delta G_{sol,polar}$	$\Delta G_{sol,non-polar}$	$\Delta G_{bind}^{MM/PBSA}$
BNB/βCD									
B-form	–17.65 ± 1.84	–28.42 ± 6.66	–4.21 ± 3.51	13.92 ± 3.92	–2.98 ± 0.59	–4.04 ± 4.54	19.96 ± 5.27	–3.68 ± 0.68	1.31 ± 3.94
C-form	–19.85 ± 1.34	–31.76 ± 2.82	–12.95 ± 4.23	21.27 ± 3.51	–3.41 ± 0.21	–7.01 ± 2.18	27.73 ± 3.81	–4.12 ± 0.19	–1.24 ± 2.78
BNB/DMβCD									
B-form	–18.19 ± 1.06	–27.08 ± 3.65	–6.66 ± 2.59	13.65 ± 2.51	–3.23 ± 0.32	–5.14 ± 3.5	18.44 ± 3.29	–3.99 ± 0.32	–1.12 ± 3.13
C-form	ND	ND	ND	ND	ND	ND	ND	ND	ND
BNB/HPβCD									
B-form	–16.94 ± 1.88	–27.81 ± 5.95	–4.12 ± 3.49	12.30 ± 3.45	–2.88 ± 0.52	–5.58 ± 4.07	17.76 ± 4.52	–3.50 ± 0.54	–0.73 ± 3.90
C-form	–20.91 ± 2.01	–33.77 ± 2.78	–10.94 ± 3.58	16.91 ± 2.66	–3.62 ± 0.21	–10.52 ± 3.42	22.56 ± 3.10	–4.35 ± 0.17	–5.60 ± 3.38
BNB/SBEβCD									
B-form	–19.77 ± 2.24	–38.47 ± 2.69	–10.20 ± 6.69	18.11 ± 6.11	–4.28 ± 0.27	–15.06 ± 3.66	23.27 ± 6.20	–5.22 ± 0.19	–10.85 ± 3.51
C-form	–18.53 ± 2.45	–35.99 ± 3.86	–5.28 ± 5.90	15.83 ± 5.19	–3.94 ± 0.39	–10.85 ± 3.69	20.58 ± 6.02	–4.86 ± 0.39	–7.03 ± 3.77

Table 3. Apparent stability constants (K_c) of BNB inclusion complexes with βCD, HPβCD, and SBEβCD determined from phase solubility studies at 25°C, compared with reported K_c values for related compounds (PSO = psoralen, MOP = 8-methoxypsoralen).

System	Intercept	Slope	R^2	K_c (M^{-1})	Reported K_c (M^{-1})	
					PSO [34]	MOP [35]
BNB/βCD		0.0012	0.98	140	663	259
BNB/HPβCD	0.0077	0.0016	0.99	185	-	449
BNB/SBEβCD		0.002	0.96	260	-	-

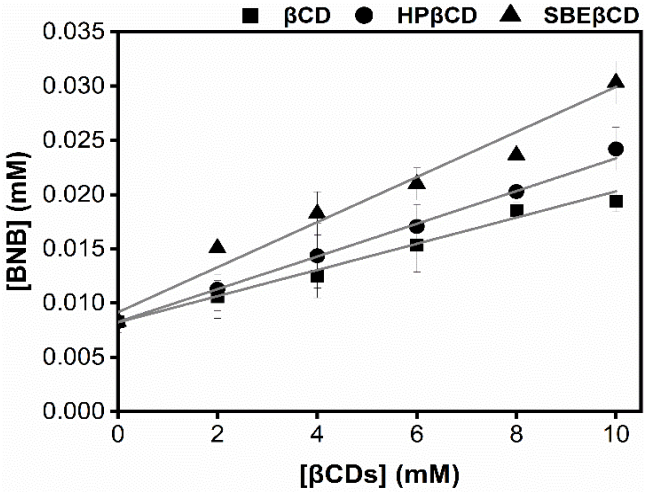

Figure 4. Phase solubility diagram of BNB in the presence of βCD (■), HPβCD (●), and SBEβCD (▲) in water at 25°C. Error bars represent the standard deviation of three independent measurements.

Data from the other four simulations are included in Supplementary Table S1. Across all systems, the entropic contribution (TΔS) is consistently negative, indicating that complex formation is accompanied by a reduction in entropy, as expected when the ligand and cyclodextrin become more constrained. This entropic penalty is most pronounced for SBEβCD, reflecting tighter host-guest complexation and reduced flexibility upon binding. Van der Waals interactions are the dominant stabilizing force in all complexes, particularly in SBEβCD and HPβCD, which correlates with strong hydrophobic interactions inside the cyclodextrin cavity. Electrostatic contributions are more variable and generally stronger in C-form orientations, highlighting the importance of ligand orientation in stabilizing the complex. Polar solvation energies ($\Delta G_{sol,polar}$) oppose binding due to desolvation effects, whereas non-polar solvation energies ($\Delta G_{sol,non-polar}$) are consistently negative, reinforcing hydrophobic stabilization. Overall, the binding free energies (ΔG_{bind}) indicate that C-form orientations generally bind more favorably than B-forms. SBEβCD shows the strongest binding affinity, followed by HPβCD, DMβCD, and βCD, reflecting the critical role of cyclodextrin derivatization and hydrophobic cavity expansion in enhancing complex stability. The variability observed across the MD trajectories underscores the dynamic nature of these host-guest systems, emphasizing the necessity of sampling multiple conformations for accurate binding estimation. BNB binding is driven predominantly by van der Waals forces and hydrophobic interactions, which are partially counteracted by entropic penalties and polar solvation energies. Among the cyclodextrins, the C-form orientations generally confer stronger binding, with SBEβCD exhibiting the highest affinity. This is attributed to its extended hydrophobic cavity, which facilitates deeper guest encapsulation and reduces solvent exposure. HPβCD and DMβCD also stabilize BNB effectively, though to a lesser extent, while native βCD demonstrates the weakest binding. Collectively, these findings highlight the critical role of both cyclodextrin derivatization and hydrophobic cavity expansion in enhancing host-guest stability.

3.5 Phase solubility analysis and stability constants

The interaction between BNB and β-cyclodextrin (βCD) derivatives was further probed using phase solubility studies in aqueous medium at 25°C, following the classical Higuchi-Connors approach [23]. Although DMβCD was included in the initial computational screening alongside βCD, HPβCD, and SBEβCD, molecular dynamics simulations revealed minimal host-guest contacts and recurrent dissociation events for the BNB/DMβCD complex, indicating poor encapsulation efficiency. Based on these computational findings, BNB/DMβCD was excluded from experimental validation, and phase solubility studies were therefore conducted for BNB/βCD, BNB/HPβCD, and BNB/SBEβCD only. As shown in Figure 4, the solubility of BNB increased linearly with

rising concentrations of all tested βCDs. Such profiles correspond to the A_L type in the Higuchi-Connors classification [29,30], indicative of 1:1 host-guest stoichiometry. Among the tested hosts, SBEβCD exhibits the steepest slope, indicating the highest complexation efficiency, followed by HPβCD and βCD. The apparent stability constants (K_c) derived from the Equation (1) showed distinct differences in complex stability. Native βCD yielded the lowest K_c (140 M^{-1}), whereas HPβCD showed moderate binding (185 M^{-1}). Notably, SBEβCD produced the highest constant (260 M^{-1}), highlighting its superior encapsulation capacity. These results demonstrate that substitution on the βCD framework enhances the binding affinity toward BNB, with the negatively charged sulfobutylether groups of SBEβCD likely providing additional electrostatic and van der Waals interactions that stabilize the complex as reported for carbamazepine, oxyresveratrol, and sorafenib [31–33]. When compared with related derivatives Table 3, the K_c of BNB/βCD is lower than that of psoralen (PSO, 663 M^{-1}) but comparable to that of 8-methoxypsoralen (MOP, 259 M^{-1}) [34,35], highlighting the influence of subtle structural modifications on host–guest recognition. While HPβCD shows higher affinity for BNB than βCD and offers established pharmaceutical safety, SBEβCD provides the strongest binding in this study. These findings, together with comparative data on psoralen derivatives, place the present results within the broader context of βCD-mediated solubilization and formulation development.

3.6 Morphological and thermal characterization

Scanning electron microscopy (SEM) was used to examine the morphological features of pure BNB, βCDs, their physical mixtures, and the corresponding inclusion complexes Figure 5. Pure BNB displayed irregular crystalline structures with uneven surfaces, whereas native βCD and DMβCD exhibited characteristic rod-like and spherical morphologies, respectively, consistent with previous reports [36]. HPβCD showed spherical particles with surface irregularities and fine pores [37], while SBEβCD appeared smooth and uniformly spherical [38]. In contrast, inclusion complexes presented marked morphological transformations. The distinctive shapes of both BNB and βCDs disappeared, giving rise to fragmented or bulkier irregular structures. While such morphological transformations may suggest interactions between BNB and βCDs, SEM analysis alone cannot confirm the formation of inclusion complexes. Therefore, these observations are considered supportive and are interpreted in conjunction with other characterization techniques. Similar SEM-based evidence of morphology loss upon complexation has been reported for other cyclodextrin systems [27,39].

Differential scanning calorimetry (DSC) was performed to assess the thermal properties of BNB, βCDs, their physical mixtures, and the inclusion complexes Figure 6. Pure BNB exhibited a sharp endothermic peak at 294.7°C, consistent with its crystalline melting point, while βCDs displayed broad endothermic transitions characteristic of their amorphous or hydrated states (128.5°C for βCD, 88.7°C for HPβCD, and 96.1°C for SBEβCD). A small endothermic peak observed around 200°C to 220°C in the BNB/βCD system is attributed to structural heterogeneity within the lyophilized complex. This thermal event likely reflects partial encapsulation of BNB, whereby an incomplete complex fraction retains residual crystallinity and exhibits a shifted melting transition. Alternatively, it may correspond to thermal reorganization of an amorphous BNB phase formed during lyophilization. The absence of this feature in BNB/HPβCD and BNB/SBEβCD systems suggests more complete and homogeneous complexation with the modified cyclodextrins.

In both the physical mixtures and lyophilized inclusion complexes, the cyclodextrin dehydration peak was observed to shift toward lower temperatures compared to the native cyclodextrins. This downward shift is attributed to processing-induced changes in the hydration state rather than reflecting weaker complexation. In the inclusion complexes, lyophilization removes or redistributes bound water molecules within the cyclodextrin cavity, resulting in loosely held residual water requiring less thermal energy for release. In the physical mixtures, mechanical mixing disrupts the cyclodextrin hydration shell at the particle surface, reducing water–cyclodextrin binding energy independently of any inclusion complex formation. In contrast, the thermograms of BNB/βCDs inclusion complexes showed disappearance or significant shifts

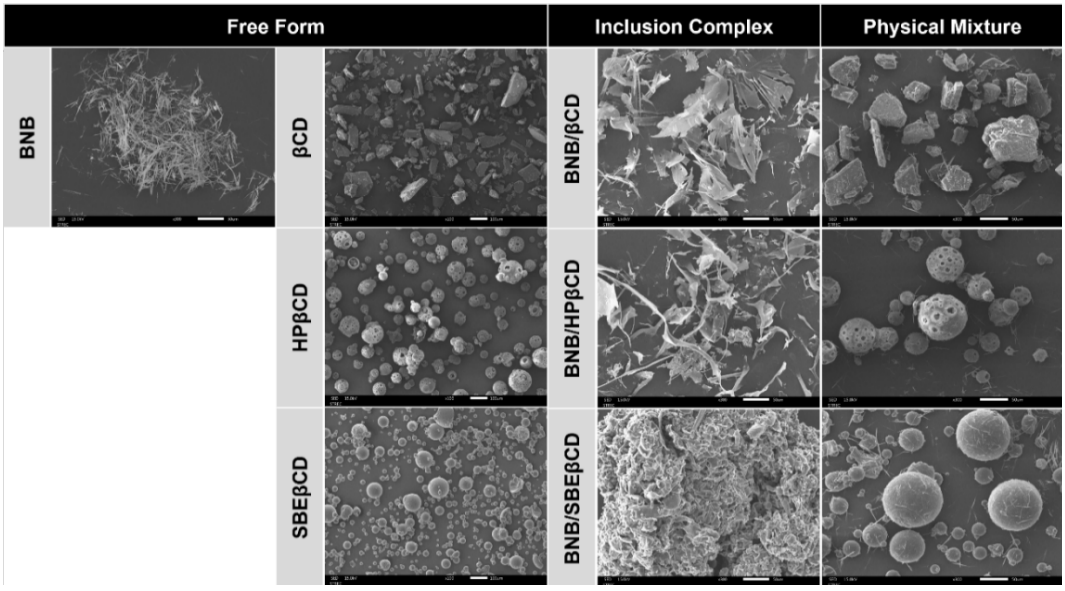

Figure 5. SEM images of free BNB, βCD, HPβCD, and SBEβCD, together with their corresponding inclusion complexes and physical mixtures.

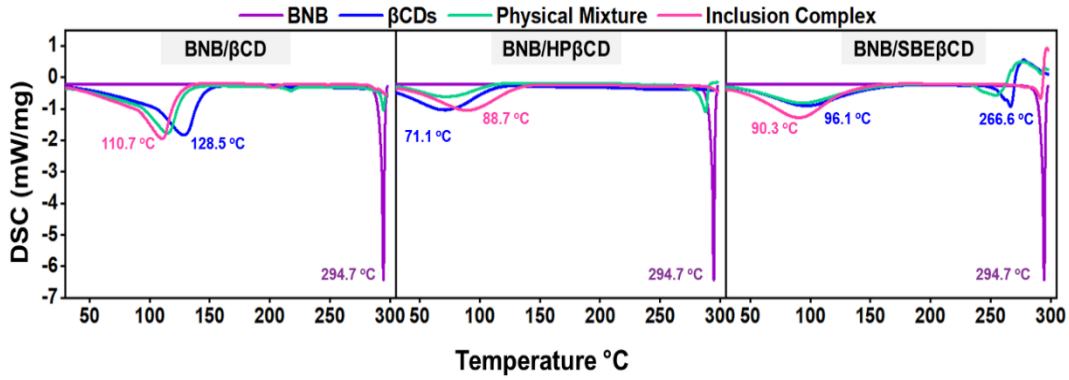

Figure 6. DSC thermograms of BNB, βCDs, their physical mixtures, and inclusion complexes: (Left) BNB/βCD, (middle) BNB/HPβCD, and (right) BNB/SBEβCD.

of BNB's melting peak, accompanied by peak broadening. Such modifications are widely recognized as indicators of successful inclusion complex formation and amorphization of the guest molecule within the host cavity [40–43]. The dehydration peak of cyclodextrins was observed to shift toward lower temperatures in both the physical mixtures and lyophilized inclusion complexes. Although an upward shift in dehydration temperature is generally associated with stronger water–cyclodextrin interactions, a downward shift indicates reduced binding energy of residual water molecules following processing. Lyophilization removes or redistributes bound water within the cyclodextrin cavity, resulting in more loosely held residual water that requires less thermal energy for release. Furthermore, partial encapsulation of BNB within the cyclodextrin cavity may displace water molecules, thereby reducing water–cyclodextrin interaction strength without reflecting a loss of complexation efficiency. Therefore, the observed downward shift in dehydration temperature is attributed to processing-induced changes in the hydration state of cyclodextrins rather than being solely indicative of interaction strength or complex stability [44]. The reduction of crystallinity in BNB suggests partial or complete encapsulation, which enhances structural disorder and further supports complexation. The DSC analysis in this study was not optimized to detect glass transition events (T_g), and therefore conclusions regarding amorphous phase formation are based on complementary evidence rather than T_g determination.

3.7 ^{1}H NMR spectroscopic analysis

BNB/βCDs (βCD, HPβCD, and SBEβCD) complexes were further characterized by ^{1}H NMR spectroscopy and compared with free BNB and the corresponding cyclodextrin hosts. Upon complexation, the ^{1}H NMR spectra of all BNB/βCDs complexes recorded in DMSO-d_6 showed noticeable peak broadening together with slight chemical shift perturbations relative to free BNB. These spectral changes indicate the formation of BNB/βCDs complexes and suggest the presence of intermolecular interactions between BNB and the cyclodextrin derivatives (Figure S1–S4). The observed peak broadening is characteristic of inclusion complex formation and can be attributed to restricted rotational and translational motion of the encapsulated BNB molecule within the cyclodextrin cavity, leading to longer tumbling correlation times and reduced molecular dynamics in solution. The consistency of these spectral features across all BNB/βCDs complexes suggests that BNB forms stable inclusion complexes regardless of the degree of CD substitution, though differences in the extent of chemical shift changes may reflect variations in binding affinity and cavity accessibility among the three hosts.

4. Conclusions

This work demonstrates that inclusion complexation with β-cyclodextrins (βCDs) markedly enhances the aqueous solubility and supports stable inclusion complex formation and supports stable inclusion complex formation of N-(4-bromobenzoyl)-8-methoxypsoralen-4-amine (BNB), a psoralen-based anti-breast cancer agent. Using a combined computational and experimental strategy, we systematically evaluated the binding modes, dynamic stability, thermodynamics, and solid-state characteristics of BNB with native βCD and its derivatives (DMβCD, HPβCD, and SBEβCD). Among these, SBEβCD emerged as the most effective host. Computationally, the BNB/SBEβCD complex was consistently the most stable, exhibiting superior dynamic retention, the highest host-guest contact density, and the most favorable binding free energy. These predictions were strongly validated by experiment: phase solubility analysis confirmed an A_L-type profile with the highest apparent stability constant, while SEM and DSC provided morphological and thermal evidence consistent with inclusion complex formation. ^{1}H NMR analysis provided additional spectroscopic evidence of BNB–cyclodextrin complex formation, as demonstrated by noticeable peak broadening and chemical shift perturbations relative to the free components. Collectively, these results provide compelling evidence that SBEβCD offers a highly efficient encapsulation environment for BNB. This integrated approach not only establishes SBEβCD as a rational carrier for BNB but also underscores its potential to advance the development of this agent as a viable chemotherapeutic candidate for breast cancer.

Acknowledgments

This research has received funding support from the National Science, Research and Innovation Fund (NSRF) via the Program Management Unit for Human Resources & Institutional Development, Research and Innovation (Grant number: B38G680006). G. B. thank the Scholarship Program for ASEAN and NON-ASEAN Countries, Graduate School, Chulalongkorn University (CU), and the 90th anniversary of CU Fund (Ratchadaphiseksomphot Endowment Fund, Grant number: GCUGR1125682070D).

References

[1] U. Veronesi, P. Boyle, A. Goldhirsch, R. Orecchia, and G. Viale, "Breast cancer," *Lancet,* vol. 365, no. 9472, p. 1727–1741, 2005.

[2] R. L. Siegel, K. D. Miller, N. S. Wagle, and A. Jemal, "Cancer statistics, 2023," *CA: A Cancer Journal for Clinicians,* vol. 73, no. 1, p. 17–48, 2023.

[3] K. Barzaman, J. Karami, Z. Zarei, A. Hosseinzadeh, M. H. Kazemi, S. Moradi-Kalbolandi, E. Safari, and L. Farahmand, "Breast cancer: Biology, biomarkers, and treatments," *International Immunopharmacology,* vol. 84, p. 106535, 2020.

[4] R. Matsuyama, S. Reddy, and T. J. Smith, "Why do patients choose chemotherapy near the end of life? A review of the perspective of those facing death from cancer," *Journal of Clinical Oncology,* vol. 24, no. 21, p. 3490–3496, 2006.

[5] K. H. Antman, P. A. Rowlings, W. P. Vaughan, C. J. Pelz, J. W. Fay, K. K. Fields C. O. Freytes, R. P. Gale, B. E. Hillner, H. K. Hollang, M. J. Kennedy, J. P. Klein, H. M. Lazarus, P. L. Mc Carthy Jr, R. Saez, G. Spitzer, E. A. Stadtmauer, S. F. Williams, S. Wolff, K. A. Sobocinski, J. O. Armitage, and M. M. Horowitz, "High-dose chemotherapy with autologous hematopoietic stem-cell support for breast cancer in North America," *Journal of Clinical Oncology,* vol. 15, no. 5, p. 1870–1879, 1997.

[6] C. Aekrungrueangkit, S. Wangngae, A. Kamkaew, R. Ardkhean, S. Thongnest, J. Boonsombat, S. Ruchirawat, and T. Khotavivattana, "Novel psoralen derivatives as anti-breast cancer agents and their light-activated cytotoxicity against HER2 positive breast cancer cells," *Scientific Reports,* vol. 12, no. 1, p. 13487, 2022.

[7] W. Saenger, "Cyclodextrin Inclusion compounds in research and industry," *Angewandte Chemie International Edition,* vol. 19, no. 5, p. 344–362, 2003.

[8] J. Szejtli, "Introduction and general overview of cyclodextrin chemistry," *Chemical Reviews,* vol. 98, no. 5, p. 1743–1754, 1998.

[9] V. Aiassa, C. Garnero, A. Zoppi, and M. R. Longhi, "Cyclodextrins and their derivatives as drug stability modifiers," *Pharmaceuticals,* vol. 16, no. 8, p. 1074, 2023.

[10] K. Kerdpol, J. Kicuntod, P. Wolschann, S. Mori, C. Rungnim, M. Kunaseth, H. Okumura, N. Kungwan, and T. Rungrotmongkol, "Cavity closure of 2-hydroxypropyl-beta-cyclodextrin: Replica exchange molecular dynamics simulations," *Polymers (Basel),* vol. 11, no. 1, p. 145, 2019.

[11] E. M. M. Del Valle, "Cyclodextrins and their uses: A review. *Process Biochemistry,* vol. 39, no. 9, p. 1033–1046, 2004.

[12] S. Tommasini, D. Raneri, R. Ficarra, M. L. Calabro, R. Stancanelli, and P. Ficarra, Improvement in solubility and dissolution rate of flavonoids by complexation with beta-cyclodextrin," *Journal of Pharmaceutical and Biomedical Analysis,* vol. 35, no. 2, p. 379–87, 2004.

[13] G. Astray, C. Gonzalez-Barreiro, J. C. Mejuto, R. Rial-Otero, and J. Simal-Gándara, "A review on the use of cyclodextrins in foods," *Food Hydrocolloids,* vol. 23, no. 7, p. 1631–1640, 2009.

[14] M. J Frisch, G. W Trucks, H. B Schlegel, G. E Scuseria, M. A Robb, J. R Cheeseman, G Scalmani, V Barone, G. A Petersson, H. Nakatsuji, X. Li, M. Caricato, A.V. Marenich, J. Bloino, B.G. Janesko, R. Gomperts, B. Mennucci, H. P. Hratchian, J.V. Ortiz, A. F. Izmaylov, J. L. Sonnenberg, D. Williams-Young, F. Ding, F. Lipparini, F. Egidi, J. Goings, B. Peng, A. Petrone, T. Henderson, D. Ranasinghe, V. G. Zakrzewski, J. Gao, N. Rega, G. Zheng, W. Liang, M. Hada, M. Ehara, K. Toyota, R. Fukuda, J. Hasegawa, M. Ishida, T. Nakajima, Y. Honda, O. Kitao, H. Nakai, T. Vreven, K. Throssell, J. A. Montgomery Jr, J. E. Peralta, F. Ogliaro, M. J. Bearpark, J. J. Heyd, E. N. Brothers, K. N. Kudin, V. N. Staroverov, T. A. Keith, R. Kobayashi, J. Normand, K. Raghavachari, A. P. Rendell, J. C. Burant, S. S. Iyengar, J. Tomasi, M. Cossi, J. M. Millam, M. Klene, C. Adamo, R. Cammi, J. W. Ochterski, R. L. Martin, K. Morokuma, O. Farkas, J. B. Foresman, and D. J. Fox, "Gaussian 16 Rev. C.01," *Wallingford CT,* no. 421, 2016.

[15] *Marvin. 23.14.0*. (2023).

[16] A. Oo, P. Mahalapbutr, K. Krusong, P. Liangsakul, S. Thanasan-surapong, V. Reutrakul, C. Kuhakarn, P. Maitarad, A. Silsirivanit, P. Wolschann, S. Putthisen, K. Kerdpol, and T. Rungrotmongkol, "Inclusion complexation of emodin with various β-cyclodextrin derivatives: Preparation, characterization, molecular docking, and anticancer activity," *Journal of Molecular Liquids*, vol. 367, Art. no. 120314, 2022.

[17] H. M. A. D. A. Case, K. A. A. Belfon, I. Y. Ben-Shalom, J. T. Berryman, S. R. Brozell, D. S. Cerutti, *et al.,*, "Amber 2022," 2022.

[18] K. N. Kirschner, A. B. Yongye, S. M. Tschampel, J. Gonzalez-Outeirino, C. R. Daniels, B. L. Foley, and R. J. Woods, "GLYCAM06: A generalizable biomolecular force field," *Journal of Computational Chemistry,* vol. 29, no. 4, p. 622–655, 2008.

[19] J. Wang, R. M. Wolf, J. W. Caldwell, P. A. Kollman, and D. A. Case, "Development and testing of a general amber force field. *Journal of Computational Chemistry,* vol. 25, no. 9, p. 1157–1174, 2004.

[20] W. L. Jorgensen, J. Chandrasekhar, J. D. Madura, R. W. Impey, and M. L. Klein, "Comparison of simple potential functions for simulating liquid water," *Journal of Computational Physics,* vol. 79, no. 2, p. 926–935, 1983.

[21] J. Ryckaert, G. Ciccotti, and H. J. C. Berendsen, "Numerical integration of the cartesian equations of motion of a system with constraints: molecular dynamics of n-alkanes," *Journal of Computational Physics,* vol. 23, no. 3, p. 327–341, 1977.

[22] D. M. York, T. A. Darden, and L. G. Pedersen, "The effect of long-range electrostatic interactions in simulations of macro-molecular crystals: A comparison of the Ewald and truncated list methods," *Journal of Computational Physics,* vol. 99, no. 10, p. 8345–8348, 1993.

[23] T. Higuchi, and A. L. Connors, "Phase solubility techniques," *Advances in Analytical Chemistry and Instrumentation,* vol. 4, pp. 117–212, 1965.

[24] J. A. Kamimura, E. H. Santos, L. E. Hill, and C. L. Gomes, "Antimicrobial and antioxidant activities of carvacrol micro-encapsulated in hydroxypropyl-beta-cyclodextrin," *LWT - Food Science and Technology,* vol. 57, no. 2, p. 701–709, 2014.

[25] C. S. Marques, S. G. Carvalho, L. D. Bertoli, J. C. O. Villanova, P. F. Pinheiro, D. C. M. Dos Santos, M. I. Yoshida, J. C. C. de Freitas, D. F. Cipriano, and P. C. Bernardes, "β-Cyclodextrin inclusion complexes with essential oils: Obtention, characterization, antimicrobial activity and potential application for food preservative sachets," *Food Research International,* vol. 119, p. 499–509, 2019.

[26] C. Preuksarattanawut, W. Mangmee, M. Prousoontorn, E. Nisarattanaporn, and K. Siraleartmukul, "Enhancing stability and antioxidant efficacy of fisetin by encapsulating as β-cyclodextrin inclusion complex with porous polylactic acid film from breath figure," *Journal of Metals, Materials and Minerals,* vol. 31, no. 1, 2021.

[27] N. Yasuda, S. Ali, A. Aman, K. Krusong, N. Herfindo, W. Chavasiri, K. Choowongkomon, P. Wolschann, P. Mahalapbutr, T. Rungrotmongkol, and S. Hannongbua, "*In vitro* and in silico studies of the inclusion complexation of 8-bromobaicalein with beta-cyclodextrins," *Journal of Molecular Graphics and Modelling,* vol. 132, p. 108840, 2024.

[28] S. Ali, P. Saokaew, A. Aman, D. Todsaporn, K. Sanachai, K. Krusong, S. Hannongbua, P. Eolscann, P. Mahalapbutr, and T. Rungrotmongkol, "Enhancing solubility and stability of piperine using beta-cyclodextrin derivatives: computational and experimental investigations," *Journal of Biomolecular Structure and Dynamics,* vol. 43, no. 5, p. 2596–2609, 2025.

[29] J. He, Z. P. Zheng, Q. Zhu, F. Guo, and J. Chen, "Encapsulation mechanism of oxyresveratrol by β-cyclodextrin and hydroxypropyl-beta-cyclodextrin and computational analysis," *Molecules,* vol. 22, no. 11, 2017.

[30] A. Matencio, F. Garcia-Carmona, and J. M. Lopez-Nicolas, "The inclusion complex of oxyresveratrol in modified cyclodextrins: A thermodynamic, structural, physicochemical, fluorescent and computational study," *Food Chemistry,* vol. 232, p. 177–184, 2017.

[31] A. S. Jain, A. A. Date, R. R. Pissurlenkar, E. C. Coutinho, and M. S. Nagarsenker, "Sulfobutyl ether(7) beta-cyclodextrin (SBE(7) beta-CD) carbamazepine complex: Preparation, characterization, molecular modeling, and evaluation of in vivo anti-epileptic activity," *American Association of Pharmaceutical Scientists PharmSciTech,* vol. 12, no. 4, p. 1163–75, 2011.

[32] S. Ali, A. Aman, K. Hengphasatporn, L. Oopkaew, B. Todee, R. Fujiki, *et al.*, Evaluating solubility, stability, and inclusion complexation of oxyresveratrol with various beta-cyclodextrin derivatives using advanced computational techniques and experimental validation. *Computational Biology and Chemistry,* vol. 12, p. 108111, 2024.

[33] A. Aman, S. Ali, P. Mahalapbutr, K. Krusong, P. Wolschann, and T. Rungrotmongkol, "Enhancing solubility and stability of sorafenib through cyclodextrin-based inclusion complexation: in silico and *in vitro* studies," *RSC Advances,* vol. 13, no. 39, p. 27244–27254, 2023.

[34] F. F. Vincieri, G. Mazzi, N. Mulinacci, M. Bambagiotti-Alberti, F. Dall' Acqua, and D. Vedaldi, "Improvement of dissolution characteristics of psoralen by cyclodextrins complexation," *Farmaco,* vol. 50, no. 7-8, p. 543–547, 1995.

[35] R. D. Machado, J. C. G. Silva, L. A. D. Silva, G. A. R. Oliveira, L. M. Liao, E. M. Lima, M. C. de Morais, E. C. da Conceicao, and K. R. Rezende, "Improvement in solubility-permeability Interplay of psoralens from brosimum gaudichaudii plant extract upon complexation with hydroxypropyl-beta-cyclodextrin," *Molecules,* vol. 27, no. 14, 2022.

[36] P. Mahalapbutr, K. Thitinanthavet, T. Kedkham, H. Nguyen, L. t. h. Theu, S. Dokmaisrijan, L. Huyuh, N. Kungwan, and T. Rungrotmongkol, "A theoretical study on the molecular encapsulation of luteolin and pinocembrin with various derivatized beta-cyclodextrins," *Journal of Molecular Structure,* vol. 1180, p. 480–490, 2019.

[37] S. Li, L. Yuan, Y. Chen, W. Zhou, and X. Wang, "Studies on the inclusion complexes of daidzein with beta-cyclodextrin and derivatives," *Molecules,* vol. 22, no. 12, 2017.

[38] A. Aman, S. Ali, L. Oopkaew, P. Mahalapbutr, A. Ismail, K. Krusong, P. Wolschann, and T. Rungrotmongkol, "Inclusion complexes of regorafenib with beta- and gamma-cyclodextrin derivatives: In silico and *in vitro* studies," *Journal of Molecular Liquids,* vol. 411, 2024.

[39] D. Wang, G. Chen, and L. Ren, "Preparation and characterization of the sulfobutylether-beta-cyclodextrin inclusion complex of amiodarone hydrochloride with enhanced oral bioavailability in fasted state," *American Association of Pharmaceutical Scientists PharmSciTech,* vol. 18, no. 5, p. 1526–1535, 2017.

[40] P. Mura, "Analytical techniques for characterization of cyclodextrin complexes in the solid state: A review," *Journal of Pharmaceutical and Biomedical Analysis,* vol. 113, p. 226–238, 2015.

[41] F. Giordano, C. Novak, and J. R. Moyano, "Thermal analysis of cyclodextrins and their inclusion compounds. *Thermochimica Acta,* vol. 380, no. 2, p. 123–151, 2001.

[42] W. Sangpheak, J. Kicuntod, R. Schuster, T. Rungrotmongkol, P. Wolschann, N. Kungwan, H. Viernstein, M. Mueller, and P. Pongsawasdi, "Physical properties and biological activities of hesperetin and naringenin in complex with methylated beta-cyclodextrin," *The Beilstein Journal of Organic Chemistry,* vol. 11, p. 2763–2773, 2015.

[43] J. Kicuntod, K. Sangpheak, M. Mueller, P. Wolschann, H. Viernstein, S. Yanaka, K. Kato, W. Chavasiri, P. Pongsawasdi, N. Kungwan, and T. Rungrotmongkol, "Theoretical and experimental studies on inclusion complexes of pinostrobin and beta-cyclodextrins," *Scientia Pharmaceutica,* vol. 86, no. 1, 2018.

[44] A. K. Gatiatulin, I. A. Grishin, A. V. Buzyurov, T. A. Mukhametzyanov, M. A. Ziganshin, and V. V. Gorbatchuk, "Determination of melting parameters of cyclodextrins using fast scanning calorimetry," *International Journal of Molecular,* vol. 23, no. 21, 2022.